Silicon defects in diamond

C. D. Clark
J. J. Thomson Physical Laboratory, University of Reading, Reading, Berks RG6 2AF, United Kingdom

H. Kanda
National Institute for Research in Inorganic Materials, 1-1 Namiki, Tsukuba, Ibaraki 305, Japan

I. Kiflawi and G. Sittas
J. J. Thomson Physical Laboratory, University of Reading, Reading, Berks RG6 2AF, United Kingdom
(Received 19 December 1994)

Synthetic diamonds have been grown from metal melts containing silicon, at high pressures and high temperatures. The absorption and photoluminescence spectra have been investigated in the temperature range 1.8–77 K. A 12-line fine structure is observed close to 1.682 eV, and this can be divided into three similar groups each containing four components. The relative strengths of the optical absorption for the three groups of lines are found to be the same as the ratio of the abundancies of the natural isotopes of silicon, ^{28}Si, ^{29}Si, and ^{30}Si, thus showing that the 1.682-eV center is related to silicon impurity. The changes in the relative intensities of the four component lines associated with ^{28}Si indicate that the center has two ground-state energy levels with a separation of 0.20 meV. The occupancies of the two excited-state levels of separation 1.07 meV tend to reach thermal equilibrium after optical excitation and before luminescence takes place. The relative transition probabilities for the transitions have been determined. The degeneracies of the ground-state levels are the same, and the degeneracies of the excited-state levels are also equal to one another. The behavior of the 1.682-eV defect after electron irradiation and subsequent heat treatment is described.

INTRODUCTION

The wide variety of optical spectra of diamonds indicates the presence and importance of chemical impurities in diamond. Nitrogen and boron dominated the literature in the early stages. A comprehensive survey of the impurities present in natural diamonds, together with an indication of the proportions involved, was given by Sellschop[1] who discussed the detection of as many as 58 elements, mostly by nuclear probe techniques. The identification of particular characteristics with a specific impurity is not necessarily straightforward with such a wide range of possibilities. The situation is further complicated if the impurity is present in more than one defect. Nitrogen, for instance, is now well known to exist in several different configurations depending upon the earlier heat treatments it has experienced.

Vavilov *et al.*[2] reported a line at 1.684 eV in the cathodoluminescence spectrum of polycrystalline diamond prepared by chemical vapor deposition (CVD). Zaitsev, Vavilov, and Gippius[3] suggested that this line was possibly associated with the presence of silicon, because the line was also detected in a single crystal of diamond which had been subjected to silicon ion implantation. Clark and Dickerson[4] and Collins, Kamo, and Sato[5] also reported a line at 1.681 eV in the photoluminescence and absorption spectrum of diamond after ion implantation and heat treatment. Ion implantation inevitably introduces irradiation damage, and some reports in the literature[6,7] confused the 1.681-eV center with the neutral vacancy in diamond, which also shows a spectral line close by in this region of the spectrum. Collins *et al.*[8] studied the thermal annealing behavior of electron-irradiated CVD diamond, and showed that as the neutral vacancy becomes mobile the strength of the 1.681-eV absorption line increases. Measurements of the temperature dependence of the luminescence intensity of the 1.681-eV system have been reported by Collins *et al.*[8] and by Feng and Schwartz.[9]

The present paper reports an unambiguous identification of silicon impurity for the defect center associated with the 1.681-eV line in diamond. In this study single-crystal diamonds have been prepared by growth from nickel or cobalt alloy melts which had been doped with silicon.

EXPERIMENTAL DETAILS

Spectroscopic measurements were made with a SPEX 1400 double-grating monochromator using 1200-lines mm^{-1} gratings in first order. The monochromator was operated at a scanning speed of 0.1 wave numbers per second. The reproducibility of a given spectral line position over several measurements was ± 0.5 cm^{-1}. The photon-counting detector system had an integrating counting period of 1 s.

Photoluminescence spectra were excited either by an argon-ion laser beam at a power density of 400 mW mm^{-2} or by a helium-neon laser beam at a power of 30 mW mm^{-2}.

For measurements above 5 K the samples were mounted in an Oxford Instruments CF 1204 continuous-flow

helium cryostat having a thermocouple in close proximity to the sample under test. For measurements below 5 K we are indebted to Dr. A. T. Collins and L. Allers of the Physics Department at King's College London for the use of a cryostat in which the sample is immersed in liquid helium, different sample temperatures being achieved by controlling the gas pressure above the helium liquid.

Photoluminescence spectroscopy was used to investigate the spectral behavior of a diamond after electron irradiation and a series of heat treatments. The intensity of the first-order diamond Raman line was used after each treatment, to normalize the spectra, thus enabling semiquantitative comparisons between spectra to be made. The phrase normalized intensity will be used to mean the luminescence intensity relative to the integrated intensity of the diamond Raman line measured under the same conditions.

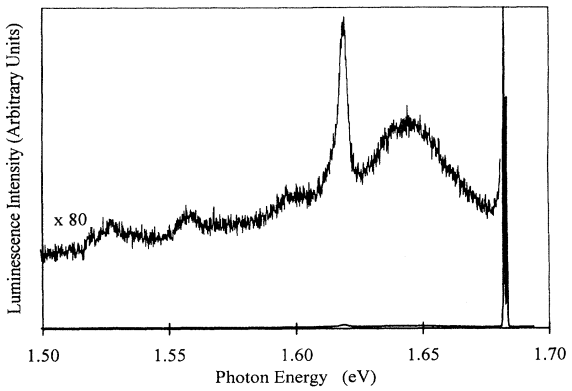

FIG. 2. Vibronic sideband structure in photoluminescence for the 1.682-eV center. The spectrum was measured at 77 K, and the sideband structure intensity has been multiplied a hundredfold with respect to the zero-phonon portion of the spectrum.

RESULTS

The photoluminescence spectrum recorded at 77 K between 1.64 and 1.70 eV for an as-grown CVD polycrystalline diamond film is shown in Fig. 1. There is an asymmetrically shaped line close to 1.680 eV having a full width at half maximum intensity of 16.8 meV. After thermal annealing at 2200 °C for 1 h at a pressure of 8 GPa, the line shifted to 1.6830 eV and had a half-width of 8.4 meV.

For comparison Fig. 1 also shows the photoluminescence spectrum recorded at 77 K with 488-nm excitation for a single-crystal diamond grown from a nickel melt at a temperature of 1500 °C and a pressure of 6 GPa. The spectrum shows the presence of two component lines at 1.6827 and 1.6837 eV. Associated with these lines there is a vibronic sideband structure which is illustrated in Fig. 2. This sideband is very similar to that which was observed in CVD polycrystalline diamond by Clark and Dickerson,[4] and it is concluded that the CVD and single-crystal luminescence lines shown in Fig. 1 are associated with the same defect. For a single-crystal diamond the combined integrated intensity of the photoluminescence lines at 1.6827 and 1.6837 eV has been determined relative to the integrated intensity of the first-order diamond Raman line at 77 K. Figure 3 shows how this normalized intensity of the lines changes during a series of isothermal heat treatments, each of duration 0.5 h, following an initial electron irradiation with 2.0-MeV electrons. Up to 600 °C the normalized intensity of lines is not significantly different from that measured in the as-grown crystal. There is an order-of-magnitude increase in the luminescence intensity after heating at 800 °C, followed by a decline by a factor of 4 after the 1200 °C anneal. Above 1200 °C the normalized intensity of the lines rises again. This annealing behavior is qualitatively similar to that observed for the 1.681-eV line in polycrystalline CVD diamond reported by Clark and Dickerson,[4] and provides further evidence that the luminescence features shown in Fig. 1 are associated with the same point defect.

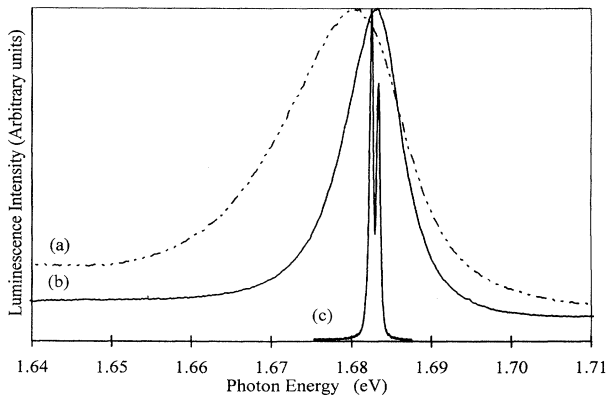

FIG. 1. Photoluminescence spectra excited by 488-nm light and measured at 77 K. Spectra are shown for (a) an as-grown CVD diamond film, (b) a CVD film after it has been heated at 2200 °C, and (c) a Si-doped single crystal.

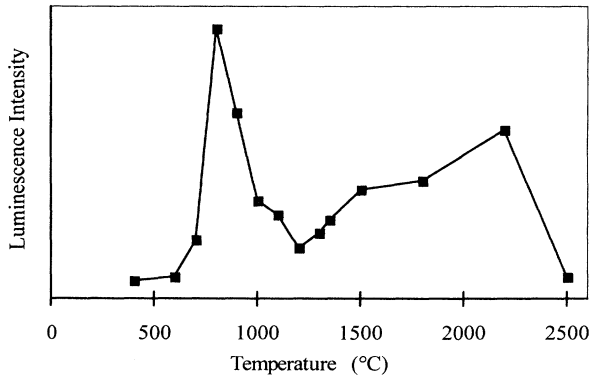

FIG. 3. Normalized luminescence of the 1.682- and 1.683-eV lines measured at 77 K after a 2.0-MeV electron irradiation (4×10^{18} electrons cm^{-2}) and subsequent thermal annealing for 0.5 h at each temperature. After some heat treatments the sample was measured several times.

Low-temperature absorption and luminescence spectra

Figure 4(a) shows the luminescence spectrum of a diamond crystal excited by 488-nm light and measured at 10 K. Similar luminescence spectra were obtained for a number of as-grown diamonds. The spectrum is comprised of 12 lines of half-widths about 0.1 meV, but this is probably instrument limited. The lines have a wide range of relative intensities. A summary of the energies of the luminescence lines measured at 30 K is given in Table I. The lines have been divided into two groups and labeled $A \rightarrow F$ and $A' \rightarrow F'$ as indicated in Fig. 4. The energy separations, ΔE between the pairs of lines $(A\text{-}A'),(B\text{-}B'). . .(F\text{-}F')$ are given in Table I, and are all close to 1.07 meV. The energy separations ΔE between the pairs of lines $(A\text{-}B)$, $(C\text{-}D)$, $(E\text{-}F)$, $(A'\text{-}B')$, $(C'\text{-}D')$, and $(E'\text{-}F')$ are also given in Table I and are close to 0.20 meV. The lines A,B and A',B' are the strongest components in their respective group, and they are the highest-energy components of each group.

Figure 4(b) shows the data points for an absorption spectrum of an as-grown synthetic diamond measured at 9 K. The absorption spectrum is rather more noisy than the luminescence spectrum, but a comparison shows that the lines present in luminescence have their counterparts in the absorption spectrum. It is concluded that each of the features included in Table I is associated with an electronic transition.

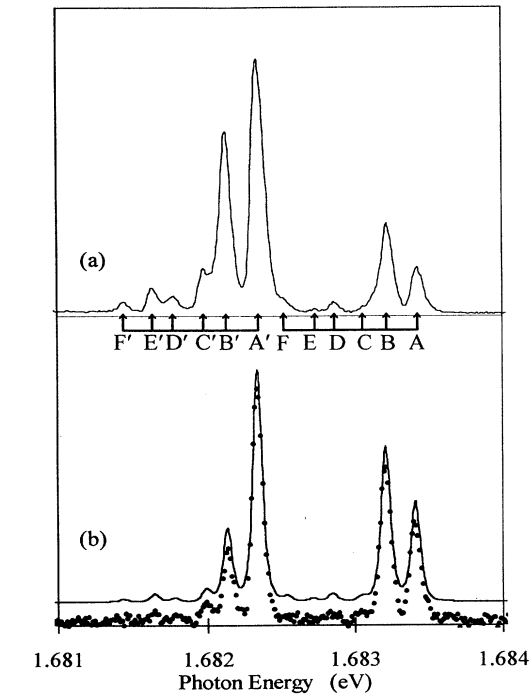

FIG. 4. (a) Photoluminescence spectrum excited by 632.8-nm light and recorded at 10 K. (b) Data points give measurements of optical absorption measured at 9 K. The full line curve represents the sum of the bi-Lorentzian line-shape contributions to give the synthesized spectrum as described in the text. The synthesized spectrum has been shifted on the ordinate axis for ease of comparison with the experimental data.

TABLE I. Energies of spectral lines and their energy separations ΔE at 30 K. Bracketed figures were the mean values from many spectra.

Line	$h\nu$ eV	Line	$h\nu$ eV	$\Delta E(\pm 0.01)$ meV	
A	1.6833(6)	A'	1.6822(8)	$A-A'=1.08$	$A-B=0.20$
B	1.6831(6)	B'	1.6820(9)	$B-B'=1.07$	$C-D=0.19$
C	1.6830(0)	C'	1.6819(4)	$C-C'=1.06$	$E-F=0.21$
D	1.6828(1)	D'	1.6817(3)	$D-D'=1.08$	$A'-B'=0.19$
E	1.6826(7)	E'	1.6815(9)	$E-E'=1.08$	$C'-D'=0.21$
F	1.6824(6)	F'	1.6813(9)	$F-F'=1.07$	$E'-F'=0.20$

Bi-Lorentzian line shapes of the form $y=\alpha/[0.20+(\nu-\nu_0)^2]^2$ have been fitted to each of the 12 lines of the absorption spectrum of Fig. 4(b), where α is chosen appropriately to fit the intensity of each line. The integrated intensity ratios A/B, C/D, and E/F are found to be equal within experimental error. The intensity ratios A'/B', C'/D', and E'/F' are also found to be nearly equal. Moreover, the integrated intensity ratios for the strongest lines in each group $B{:}D{:}F$ and $A'{:}C'{:}E'$ are both close to 92.3:4.7:3.0, which is the ratio of the isotopic natural abundances for ^{28}Si:^{29}Si:^{30}Si.

Figure 4(b) compares the measured absorption spectral data points with a spectrum synthesized from Bi-Lorentzian line shapes under the following conditions:

$$A/B=C/D=E/F, \quad A'/B'=C'/D'=E'/F' ,$$

$$A'{:}C'{:}E'=B{:}D{:}F=92.3{:}4.7{:}3.0 .$$

Such good fits of experimental and synthesized spectra have been obtained for three different samples. It is concluded that the lines A, B, A', and B' are associated with a point defect involving an atom of ^{29}Si, and that the lines (C,D,C',D') and (E,F,E',F') are similarly related to defects containing ^{28}Si and ^{30}Si, respectively.

A similar fitting of the photoluminescence spectra with different concentrations of silicon impurity has been carried out. The synthesized spectrum in this case is found to give a satisfactory representation of the experimental spectrum for samples of low overall luminescence intensity. For samples of high luminescence intensity the problem of resonance absorption has to be taken into account.

Temperature dependence of absorption

The absorption spectra have been recorded for three different diamonds as a function of temperature, and Fig. 5 illustrates the 6- and 40-K spectra. As the temperature rises the absorption line B is observed to grow at the expense of absorption line A, and similarly line B' grows at the expense of line A'.

Logarithmic plots of the ratios of the integrated absorption intensities (B'/A'), (B/A), (A/A'), and (B'/B) as a function of reciprocal temperature are presented in Figs. 6 and 7 for two diamonds. The scatter of data points arises due to the difficulty of measuring the integrated intensities of these very sharp lines, but the gradients of the best lines through the data points give the activation energies $\varepsilon_1(B/A)$, $\varepsilon_1(B'/A')$, $\varepsilon_1(A/A')$,

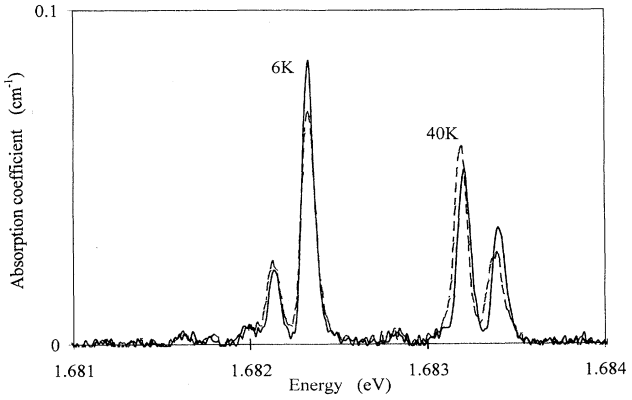

FIG. 5. Absorption spectra measured at 6 and 40 K.

and $\varepsilon_1(B/B')$ listed in Table II. The values $\varepsilon_1(B/A)$ and $\varepsilon_1(B'/A')$ compare favorably with the spectral energy separations $\Delta E(A-B)=0.20$ meV and $\Delta E(A'-B')=0.19$ meV taken from Table I.

The intercepts which the best straight lines make with ordinate axes in Figs. 6 and 7 correspond to the ratio of intensities of the absorption lines (B'/A'), (B/A), (A/A'), and (B'/B) at very high temperatures, and these are listed in Table II.

The temperature dependence of the photoluminescence spectra

The photoluminescence spectra excited by 632.8-nm light have been recorded at several temperatures in the range 1.8–60 K for three diamonds. Figure 8 shows that there is very little temperature dependence of the ratios of the intensities of the luminescence lines (A/B) and (A'/B'). The intensity ratios (A/A') and (B/B') decrease with decreasing temperature in the range 60 to 8 K, but below 5 K the intensity ratios (A/A') and (B/B') adopt values which are independent of temperature. These effects are illustrated in Figs. 9 and 10, where logarithmic plots of the ratios of intensities (A/A'), (B/B'), (B'/A'), and (B/A) as functions of $1/T$ are presented. The data for two of the samples, shown as squares and stars, are rather similar to one another, but the third sample for which the data points are triangles are significantly different. This may arise from the distortion of the luminescence spectra intensities by resonance absorption, the effect being most noticeable in samples which exhibit strong absorption lines. The absorption spectrum for the sample characterized by triangles is about 20 times stronger than the absorption of the other two samples. Provided that the absorbing centers are homogeneously distributed, then the effects of resonant absorption on the luminescence spectrum can be estimated provided the absorption spectrum is known. Such corrections have been attempted, and the results for the triangles become very similar to the other two sets of data in the temperature range 10–60 K. Notice that the triangles are found to increase their ordinate values after such a correction in Fig. 9(a), but lower their ordinate value in Fig. 9(b). This arises because line A has a weaker absorption intensity than line B, whereas line A' has a

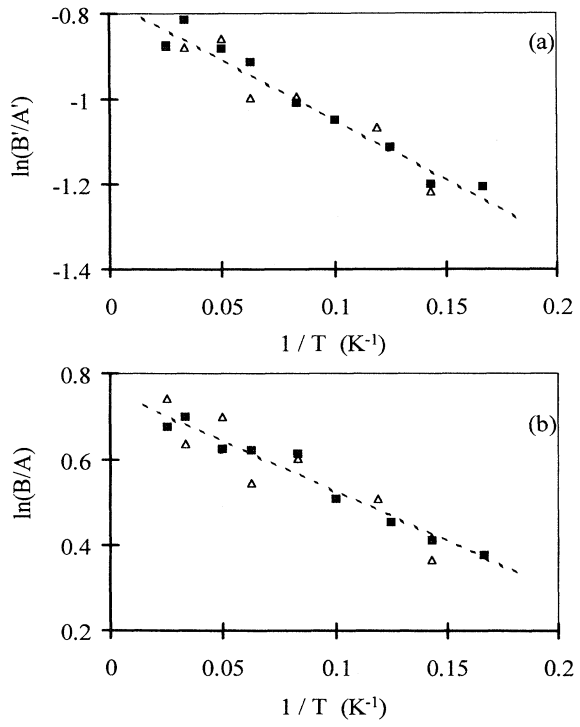

FIG. 6. Logarithmic plots of ratios of absorption line intensities (a) $\ln(B'/A')$ vs $1/T$ and (b) $\ln(B/A)$ vs $1/T$.

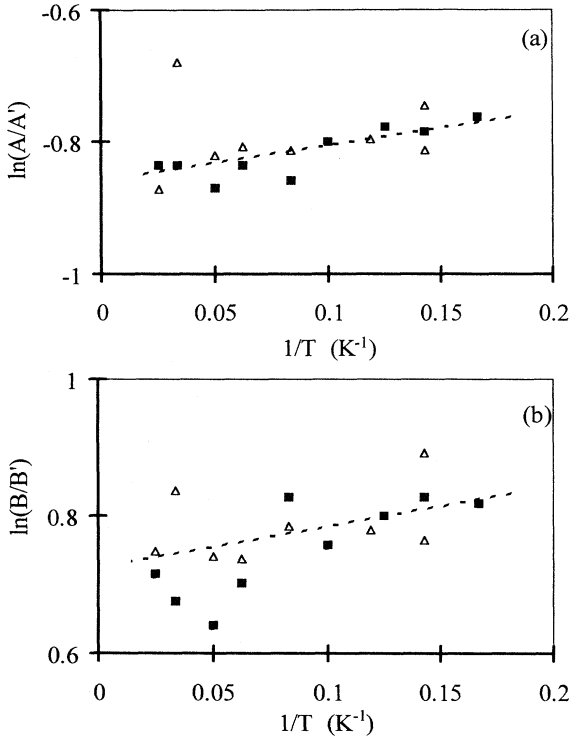

FIG. 7. Logarithmic plots of ratios of absorption line intensities (a) $\ln(A/A')$ vs $1/T$ and (b) $\ln(B/B')$ vs $1/T$.

TABLE II. Activation energies and ordinate intercepts derived from the absorption data of Figs. 6 and 7. Spectral line separations ΔE are given for comparison.

$\varepsilon_1(B/A)$ from $\ln(B/A)$ versus $(1/T)$	0.23±0.03 meV	$\Delta E(A-B)=0.20\pm0.20$ meV
$\varepsilon_1(B'/A')$ from $\ln(B'/A')$ versus $(1/T)$	0.22±0.02 meV	$\Delta E(A'-B')=0.19\pm0.02$ meV
$\varepsilon_1(A/A')$ from $\ln(A/A')$ versus $(1/T)$	−0.05±0.02 meV	
$\varepsilon_1(B/B')$ from $\ln(B/B')$ versus $(1/T)$	0.05±0.02 meV	
B'/A' from intercept	0.45±0.04	$=(b'g_2/a'g_1)$
B/A from intercept	2.25±0.06	$=(bg_2/ag_1)$
A/A' from intercept	0.43±0.06	$=(a/a')$
B'/B from intercept	0.48±0.05	$=(b'/b)$

stronger absorption intensity than line B'.

In the range of $1/T$ from 0 to 0.1 K^{-1} the best straight lines have been drawn for each of the samples through the data points of Figs. 9 and 10 to provide the activation energies ε_2 quoted in Table III. The intercepts which these lines make with the ordinate axes correspond to the appropriate ratios of luminescence intensities at very high temperatures, and these are also listed in Table III. It is seen that the activation energy $\varepsilon_2(B/B')$ and the spectral energy separation $\Delta E(B-B')$ are the same within experimental error, but $\varepsilon_2(A/A')$ is slightly lower than $\Delta E(A-A')$.

DISCUSSION

Each isotope of silicon has associated with it four electronic transitions when present in diamond. A minimum of four energy levels is necessary to describe this multiplicity of lines. The energy-level diagram shown in Fig. 11 shows two sublevels in the ground state and two levels in the excited state, together with the transitions corresponding to the lines $ABA'B'$ for the ^{28}Si defect center. The energies E, occupancies n, and degeneracies g of each of the levels are labeled on the diagram. The transition probabilities for the lines $ABA'B'$ are represented by $aba'b'$, respectively. In thermal equilibrium the ratios of the intensities of absorption then would be given by

$$(B'/A')=(n_2b'/n_1a')=(g_2b'/g_1a')\exp[(E_1-E_2)/kT]\,, \quad (1)$$

$$(B/A)=(n_2b/n_1a)=(g_2b/g_1a)\exp[(E_1-E_2)/kT]\,, \quad (2)$$

$$(A/A')=(n_1a/n_1a')=(a/a')\,, \quad (3)$$

$$(B'/B)=(n_2b'/n_2b)=(b'/b)\,. \quad (4)$$

Equations (1), (2), (3), and (4) satisfactorily account for the behavior observed in Figs. 6(a) and 6(b) and 7(a) and 7(b), respectively, the fitting parameters being set out in Table II.

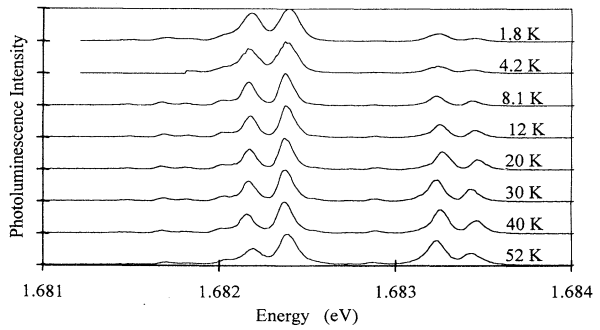

FIG. 8. Photoluminescence spectra measured at different temperatures.

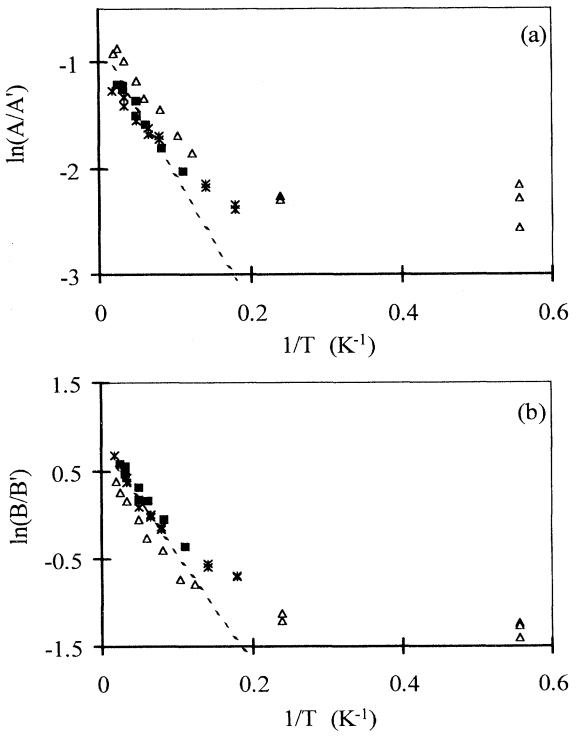

FIG. 9. Logarithmic plots of ratios of luminescence line intensities (a) $\ln(A/A')$ vs $1/T$ and (b) $\ln(B/B')$ vs $1/T$.

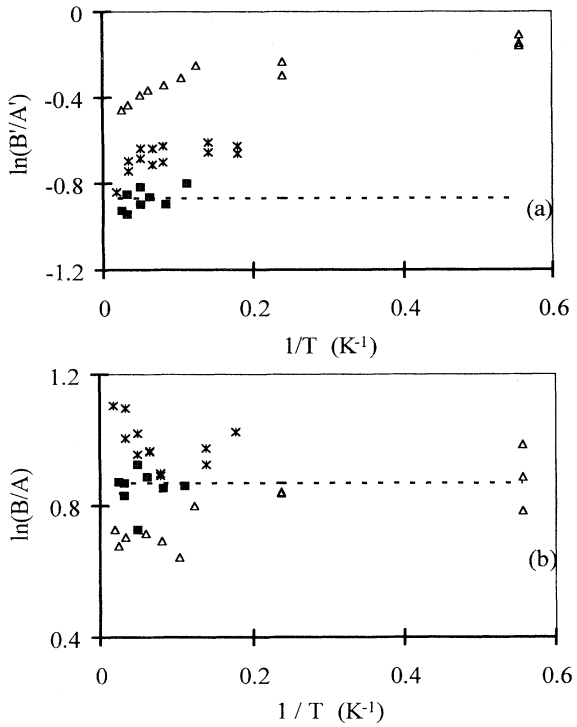

FIG. 10. Logarithmic plots of ratios of luminescence line intensities (a) $\ln(B'/A')$ vs $1/T$ and (b) $\ln(B/A)$ vs $1/T$.

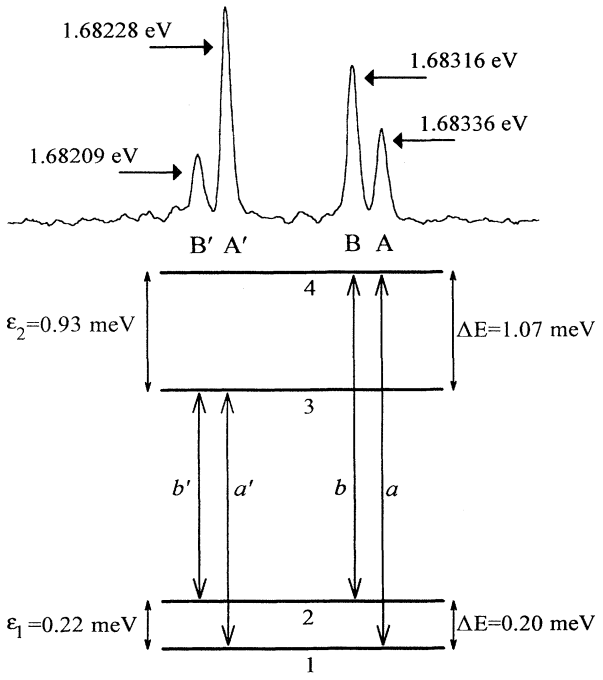

FIG. 11. Proposed energy-level diagram.

For the photoluminescence behavior it is assumed that, after optical excitation, thermal equilibrium is established between the levels of the excited state before luminescence occurs. Moreover, the transition probabilities for the luminescence lines are the same as those for the corresponding absorption lines. The ratios of luminescence intensity then would be given by

$$(B/B')=(bn_4/b'n_3)=(bg_4/b'g_3)\exp[(E_3-E_4)/kT]\ , \tag{5}$$

$$(A/A')=(an_4/a'n_3)=(ag_4/a'g_3)\exp[(E_3-E_4)/kT]\ , \tag{6}$$

$$(B'/A')=(b'n_3/a'n_3)=(b'/a')\ , \tag{7}$$

$$(B/A)=(bn_4/an_4)=(b/a)\ . \tag{8}$$

Equations (5), (6), (7), and (8) have been used to describe the behavior observed in Figs. 9 and 10 in the range of $1/T$ from 0 to 0.1 K^{-1}. The fitting parameters for each of three samples are set out in Table III. The parameters for samples $K4$ and $K16$ are reasonably consistent with one another.

By applying Eqs. (1)–(8) to the data of Tables II and III, several values for the ratios of transition probabilities and of degeneracies can be calculated, the mean values of these for $K4$ and $K16$ are $(a/b)=0.40\pm0.04$, $(b'/a')=0.44\pm0.03$, $(a/a')=0.43\pm0.06$, $(b'/b)=0.48\pm0.05$, $(g_2/g_1)=1.03\pm0.16$, and $(g_4/g_3)=0.90$

TABLE III. Activation energies and ordinate intercepts derived from the photoluminescence data of Figs. 9 and 10. Spectral line separations ΔE are given for comparison.

	Sample $K4$	Sample $K16$	Sample $K15$	
$\varepsilon_2(A/A')$ from $\ln(A/A')$ versus $1/T$	0.83±0.08	0.91±0.09	0.85±0.09	$\Delta E(A-A')=1.08\pm$ 0.02 meV
$\varepsilon_2(B/B')$ from $\ln(B/B')$ versus $1/T$	1.09±0.09	0.95±0.11	1.12±0.08	$\Delta E(B-B')=1.07\pm$ 0.02 meV
$\varepsilon_2(B'/A')$ from $\ln(B'/A')$ versus $1/T$	−0.06±0.02	−0.08±0.05	−0.22±0.03	
$\varepsilon_2(B/A)$ from $\ln(B/A)$ versus $1/T$	0.02±0.03	−0.01±0.06	−0.03±0.01	
A/A' from intercept	0.38±0.03	0.40±0.03	0.51±0.03	$=(ag_4/a'g_3)$
B/B' from intercept	0.44±0.03	0.43±0.03	0.55±0.04	$=(bg_4/b'g_3)$
B'/A' from intercept	0.48±0.03	0.40±0.03	0.57±0.02	$=(b'/a')$
A/B from intercept	0.37±0.04	0.43±0.04	0.49±0.03	$=(a/b)$

± 0.15. In view of the similarities between these ratios, the theoretical curves based upon Eqs. (1)–(8) have been added in Figs. 9 and 10, assuming that

$$(a/b)=(b'/a')=(a/a')=(b'/b)=0.44, \quad (g_4/g_3)=1$$

and

$$E_4-E_3=1.07 \text{ meV} .$$

The results of sample $K15$ (triangles in Figs. 9 and 10) are significantly different from those for $K4$ and $K16$, and there are several matters which might have to be taken into account to provide a satisfactory explanation. $K4$ and $K16$ are both as-grown samples, but $K16$ has been electron irradiated and then given a series of heat treatments up to 2200 °C, as illustrated in Fig. 3. Such a treatment could conceivably result in a different behavior for the centers before and after treatment. It certainly produces a 20-fold increase in the absorption for the silicon defect. Sample $K15$ is the only sample for which photoluminescence experiments have been extended down to a temperature of 1.8 K. In this case it seems that at very low temperatures, after optical excitation the carriers are not effectively in thermal equilibrium in the excited state of the center prior to luminescence taking place. The extent to which the mechanisms which do operate below 6 K extend to higher temperatures is not clear at this stage. More experimental work in absorption and photoluminescence at very low temperatures and upon more samples is clearly necessary.

Optical transitions between the upper sublevels of the ground and excited states of the center have the same transition probability as transition between the lower sublevels of the ground and excited states (i.e., $a'=b$). On the other hand, transitions from an upper to lower sublevel (or vice versa) between ground and excited states have a much lower transition probability (i.e., $b'=0.44a'$ or $a=0.44b$). This suggests the existence of a defect which has two similar configurations available to it, causing a doubling of the ground and excited states of the center, in turn leading to a spectral fine structure of very sharp lines. These features are rather similar to those exhibited by the ammonia molecule where the level doubling is due to a tunneling behavior between the two inversion states of the molecule. A similar tunneling process may be associated with the silicon center in diamond.

It is not easy to suggest a model for the structure of the point defect responsible for the spectral lines close to 1.682 eV at the present stage. It is clear that silicon is involved, but it is not certain how many atoms of silicon are included in each defect. The observation that the strength of the 1.682-eV lines increase in intensity after electron irradiation followed by heating at 700 °C (a temperature at which it is generally considered that the vacancy in diamond becomes mobile) could suggest that the center is a combination of a substitutional silicon atom in association with a neighboring vacant lattice site. However, it is very difficult to see how this model can be used to explain both the decline in intensity of photoluminescence in the thermal annealing range 900–1200 °C and the subsequent continuous increase in intensity in the range up to 2200 °C. A detailed study of the symmetry of the defect will probably help to resolve these difficulties.

The spectral fine structure close to 1.682 eV for the silicon defect usually is not observed in polycrystalline CVD diamond. This is probably due, at least in part, to line-broadening effects caused by the internal stress and strain distribution which is commonly present in CVD diamond films. It has been shown that a substantial reduction in line broadening for an as-grown CVD film can be achieved by heat treatment at 2200 °C. Clark and Dickerson[10] indicated that the reduction in half-width occurs progressively during a series of isothermal heat treatments from 1100 to 2200 °C. At the conclusion of these heat treatments there was still some residual line broadening, but it is not clear whether this is still due exclusively to residual internal stresses.

CONCLUSIONS

The very sharp 12-line fine structure close to 1.682 eV in diamond spectra has been divided into three identical patterns each comprising four lines. The relative intensities of these three groups is very close to 92.3:4.7:3.0, the ratio of isotopic abundances for the three naturally occurring isotopes of silicon. It is concluded that the defect center involves silicon impurity. Based upon the behavior of the center after electron irradiation and heat treatment, a defect model with a silicon atom in a substitutional lattice site accompanied by a vacancy at a neighboring lattice site can be regarded as no more than speculative at this stage of investigation.

A four-energy-level scheme, with two sublevels of separation 0.20 meV in the ground state, together with two levels of separation 1.07 meV in the excited state have been found to adequately account for the temperature dependence (between 10 and 60 K) of the relative intensities of the lines in absorption and photoluminescence. The electronic degeneracies of the two levels in the ground state are equal to one another ($g_1=g_2$), and the degeneracies of the two levels in the excited state also appear to be equal ($g_3=g_4$).

Of the four transitions possible between the doublet levels of the ground and excited states, two have a higher transition probability than the remaining pair ($a/b=0.44$), and it is suggested that this might arise from a tunneling behavior between two similar configurations of the silicon defect.

[1]J. P. F. Sellschop, in *The Properties of Diamond,* edited by J. E. Field (Academic, London, 1979).

[2]V. S. Vavilov, A. A. Gippius, B. V. Zaitsev, B. V. Deryagin, B. V. Spitsyn, and A. E. Aleksenko, Fiz. Tekh. Polopruvodn. **14**, 1811 (1980) [Sov. Phys. Semicond. **14**, 1078 (1980)]

[3]A. M. Zaitsev, V. S. Vavilov, and A. A. Gippius, Sev. Phys. Leb. Inst. Rep. **10**, 15 (1981).

[4]C. D. Clark and C. B. Dickerson, Surf. Coat. Tech. **47**, 336

(1991).
[5]A. T. Collins, M. Kamo, and Y. Sato, J. Mater. Res. **5**, 2507 (1990).
[6]L. H. Robins, E. N. Cook, E. N. Farabaugh, and A. Feldman, Phys. Rev. B **39**, 13 367 (1989).
[7]J. A. Freitas, Jr., J. E. Butler, and U. Strom, J. Mater. Res. **5**, 2502 (1990).
[8]A. T. Collins, L. Allers, C. J. H. Wort, and G. A. Scarsbrook, Diamond Relat. Mater. **3**, 932 (1994).
[9]T. Feng and D. Schwartz, J. Appl. Phys. **73**, 1415 (1993).
[10]C. D. Clark and C. B. Dickerson, Philos. Trans. R. Soc. London Ser. A **342**, 253 (1993).